Electronic Supplementary Material (ESI) for CrystEngComm.

The influence of anion, ligand geometry and stoichiometry on the structure and dimensionality of a series of Ag(I)-bis(cyanobenzyl)piperazine coordination polymers

L. J. Beeching, C. S. Hawes, D. R. Turner and S. R. Batten

Supporting Information

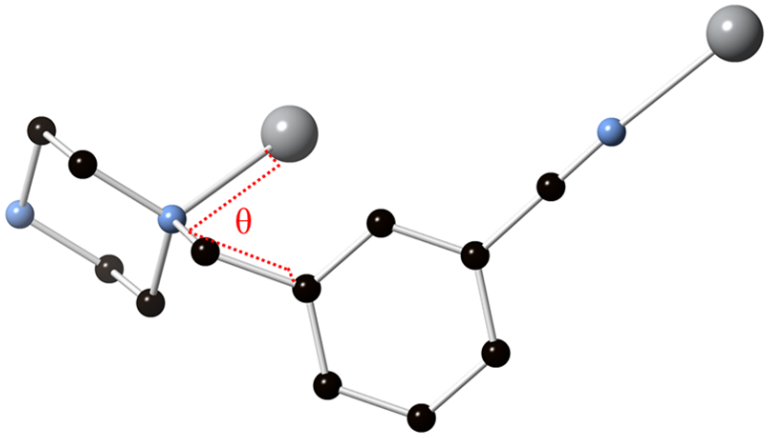

Compound	Torsion Angle θ (°)	Dimensionality
1	57.3(2)	2
2	51.8(4), 45.6(4)	2
3	50.4(2)	1
4	42.4(3)	2
5	176.9(3), 175.9(3)	3

Figure S1 Relationship between Ag-N-CH_2-C torsion angle and dimensionality of the resulting assembly

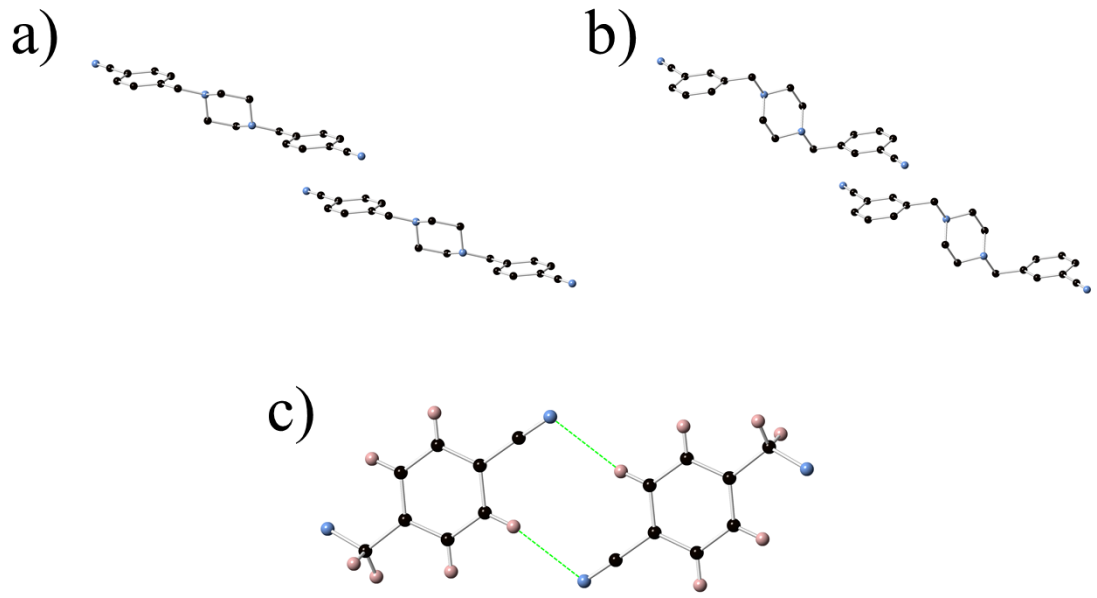

Figure S2 Intermolecular interactions in the structure of **L1** and **L2**; a) Offset face-to-face π-π interactions between molecules of **L1**; b) Offset face-to-face π-π interactions between molecules of **L2;** c) C-H···N hydrogen bonding in the structure of **L1**.

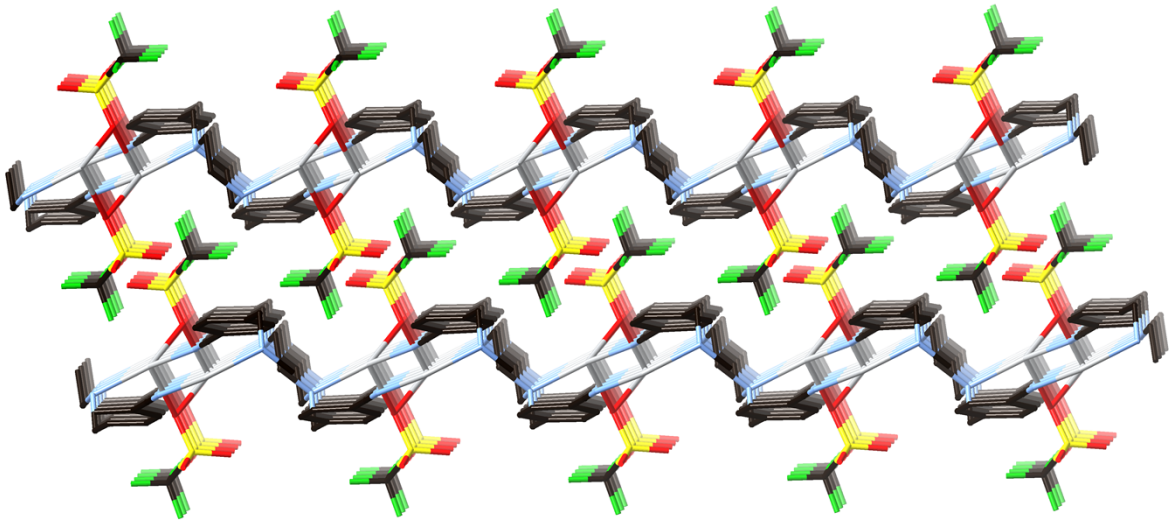

Figure S3 Crystal packing of adjacent sheets in the structure of **1**. Hydrogen atoms omitted for clarity.

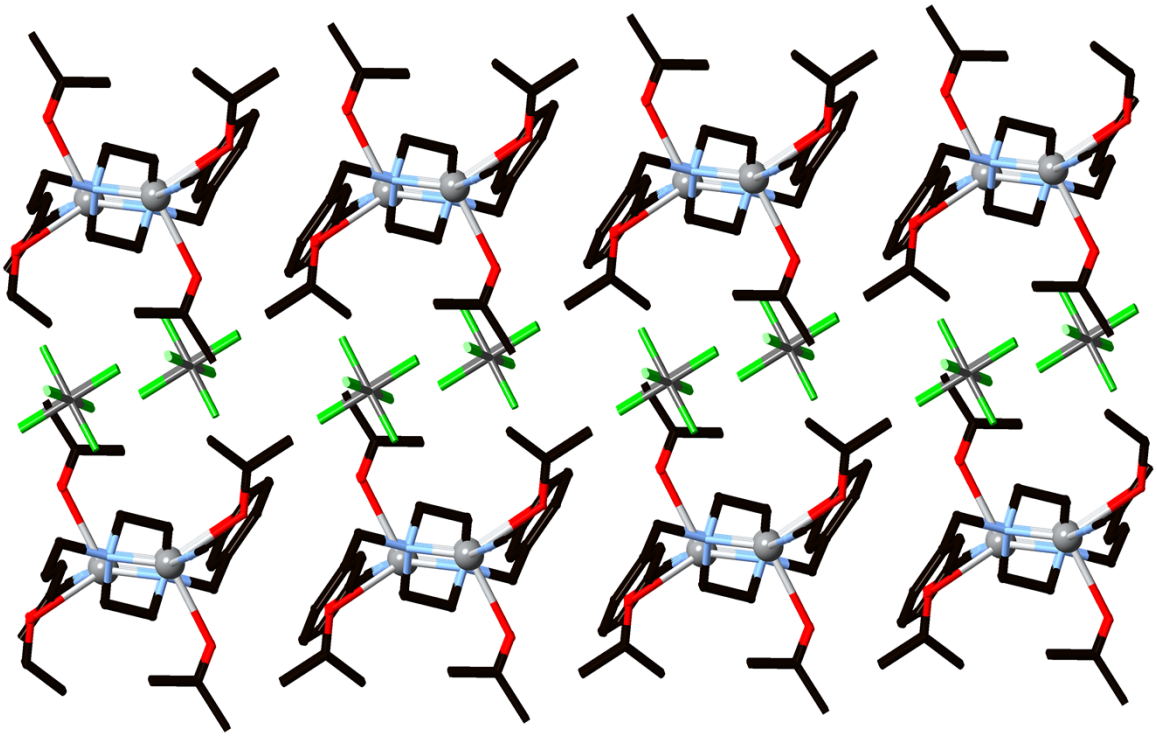

Figure S4 Crystal packing of adjacent layers of chains in the structure of **3** viewed parallel to the direction of propagation. Hydrogen atoms omitted for clarity.

X-Ray Powder Diffraction

Data collection details are provided in the X-ray crystallography section. All data collections were carried out at room temperature and compared with single crystal data collected at either 123K or 100K, leading to the expected discrepancies in exact peak positions due to thermal changes in the unit cell parameters.

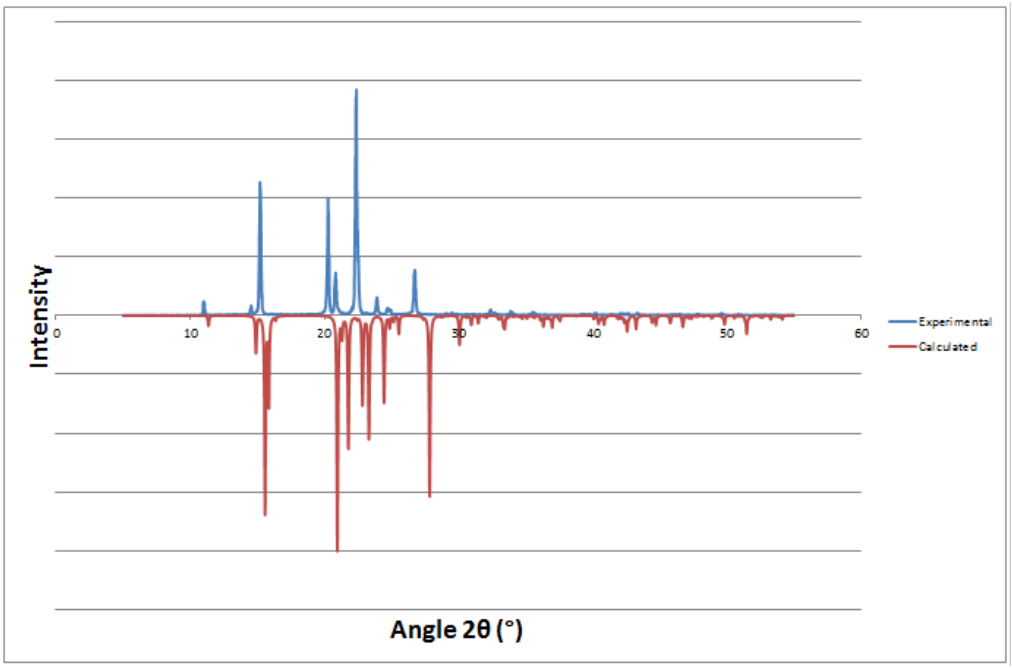

Figure S5 X-ray powder diffraction pattern for **L1**

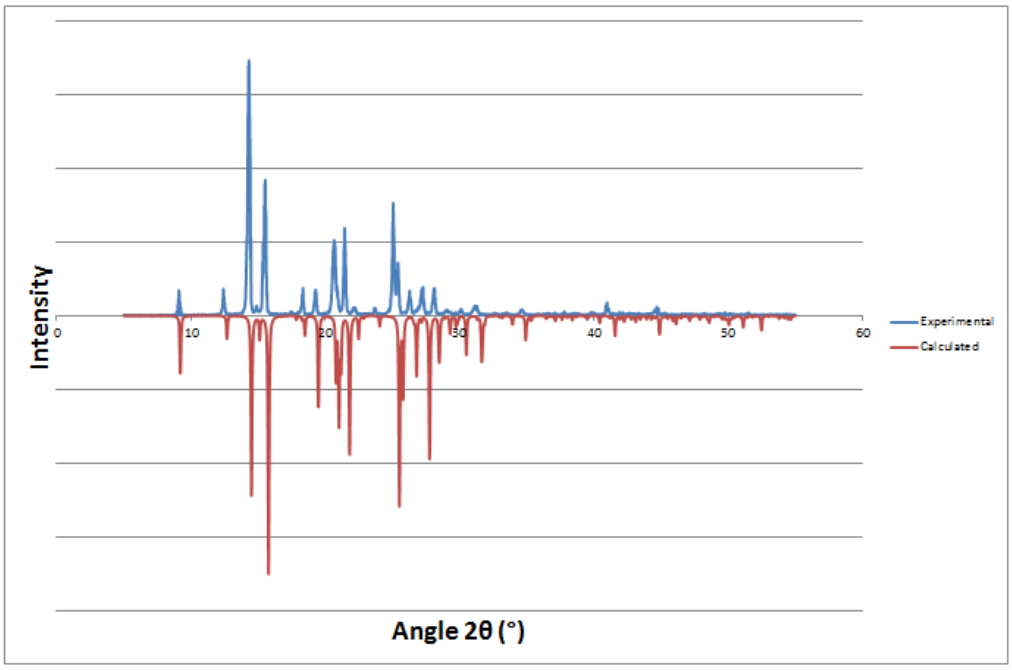

Figure S6 X-ray powder diffraction pattern for **L2**

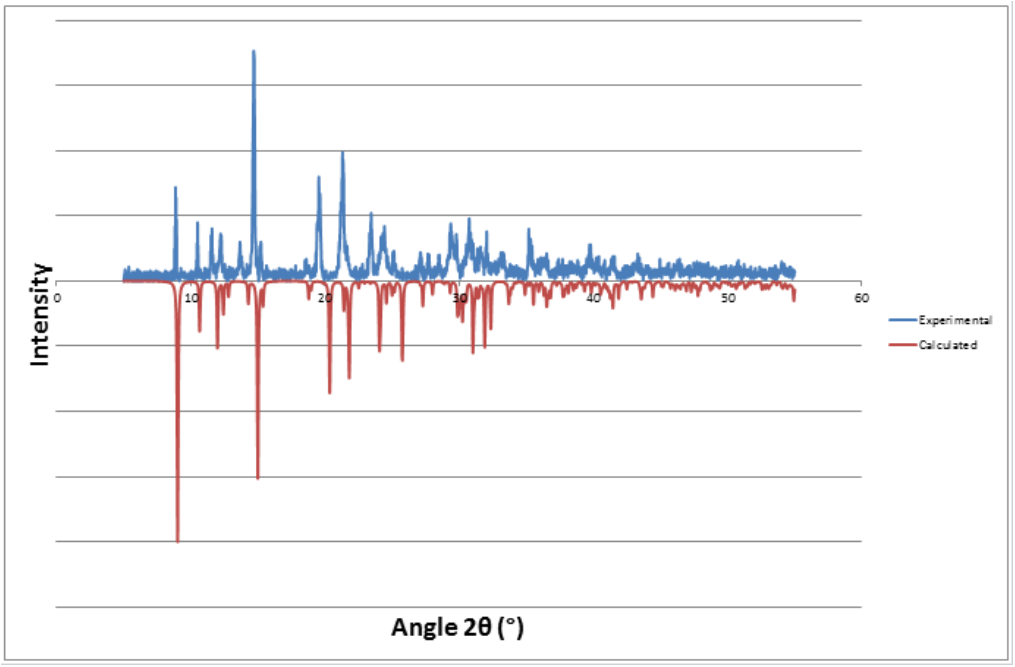

Figure S7 X-ray powder diffraction pattern for complex **1**

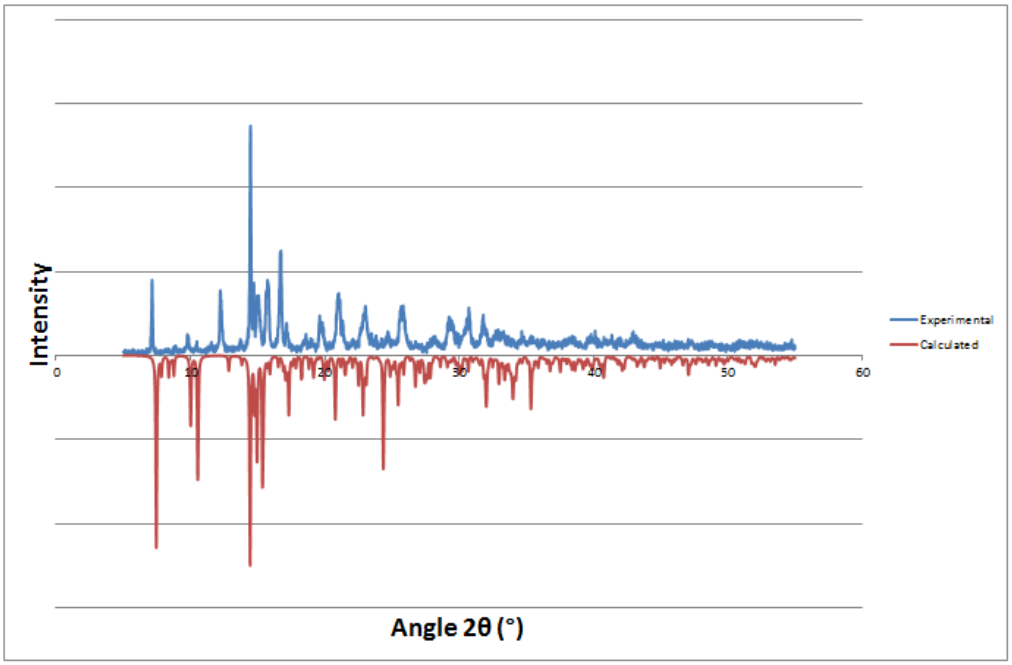

Figure S8 X-ray powder diffraction pattern for complex **2.** We ascribe the peak broadening above 2θ = 20° to partial loss of lattice solvent during the experiment.

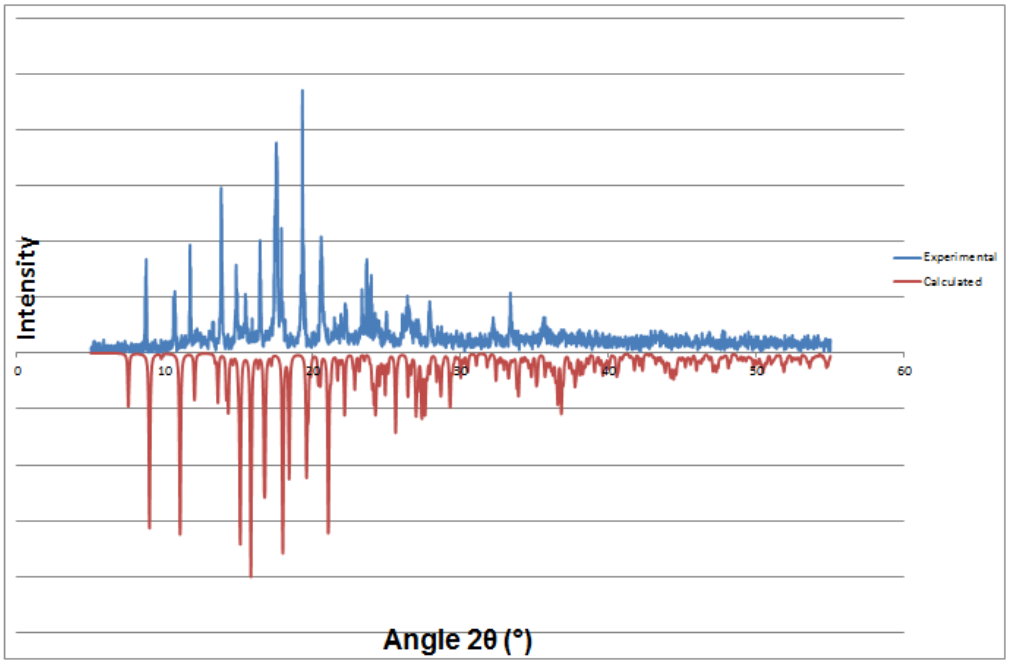

Figure S9 X-ray powder diffraction pattern for complex **3**

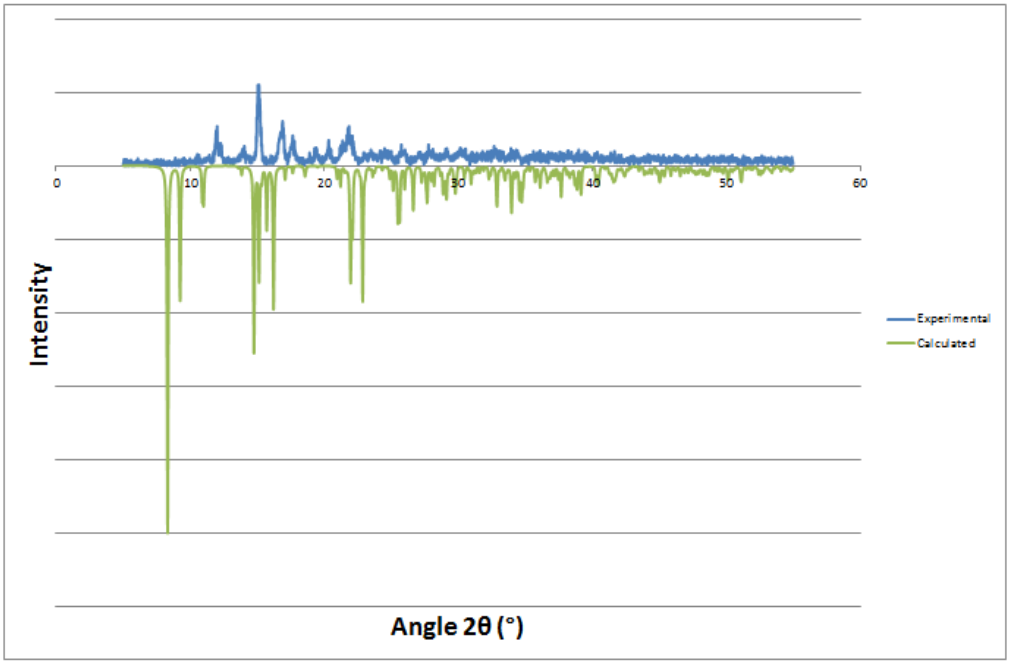

Figure S10 X-ray powder diffraction pattern for the poorly crystalline material obtained from drying complex **4**

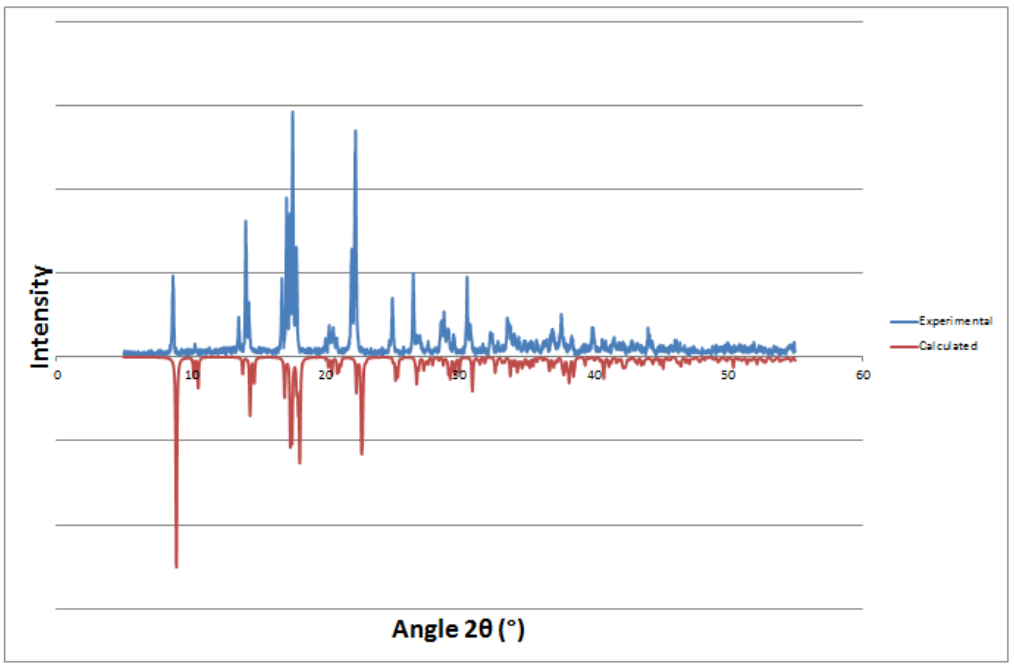

Figure S11 X-ray powder diffraction pattern for complex **5**

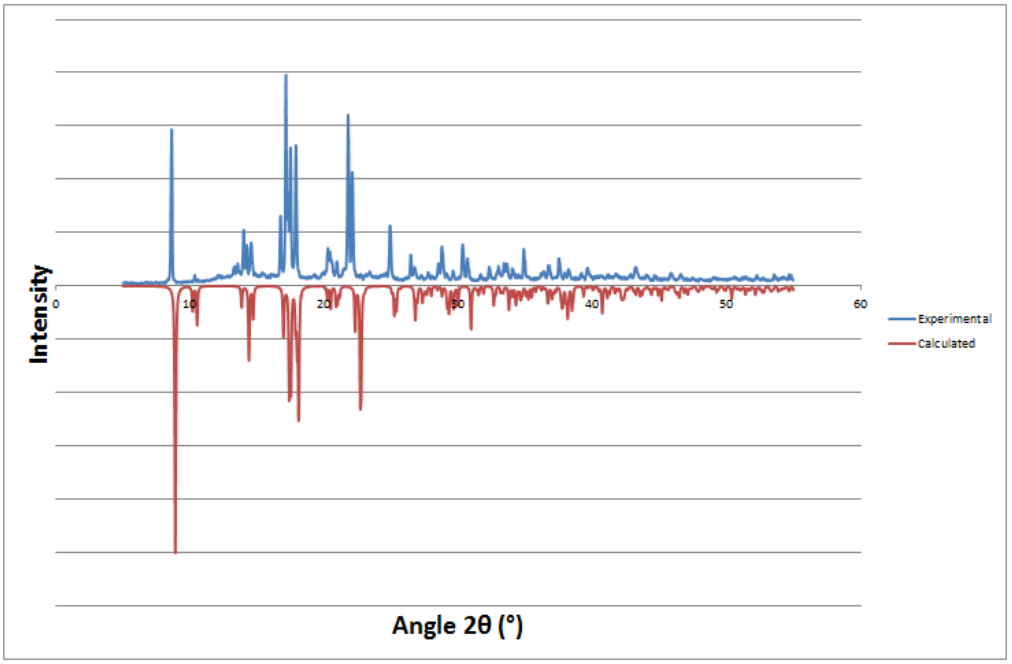

Figure S12 X-ray powder diffraction pattern for the hexafluorophosphate analogue to complex **5**, *poly*-[Ag(**L2**)]·PF_6, compared with the calculated pattern for complex **5**.